Robustness analysis of the next generation of EGR controllers in marine two-stroke diesel engines

Xavier Llamas, MSc[a*], Prof. Lars Eriksson[a]

[a]*Vehicular Systems, Dept. of Electrical Engineering, Linköping University, SE-581 83 Linköping, Sweden*
*Corresponding author. Email: xavier.llamas.comellas@liu.se

Synopsis

Exhaust Gas Recirculation (EGR) has recently been introduced in large marine two-stroke diesel engines to reduce NO_x emissions. During accelerations, controlling the amount of EGR flow while still keeping good acceleration performance can be quite challenging. The main difficulties to overcome are the delay in the scavenge receiver oxygen measurement and the upper limit in the amount of fuel that can be burned with EGR diluted air without producing black smoke. Previous oxygen feedback controllers struggled during accelerations, but a new approach to EGR control based on adaptive feedforward (AFF) has been tested successfully. Nevertheless, further analysis and tests are required before deploying the new controller to more EGR ships. A simulation platform is a great asset to test the controllers before expensive and time-limited real-world experiments have to be conducted on board of ships. With this purpose, a new EGR flow controller is introduced to track the AFF controller EGR flow setpoint in a complete ship simulation model. This new EGR controller complements the previous AFF controller and determines the control signals of the engine EGR blowers. Several acceleration scenarios are simulated, and they identify the low load area as the most challenging concerning EGR control performance due to the slower air path engine dynamics. Controller robustness in this low load area against errors in the flow estimates used by the controller is analysed. Pressure sensor bias in the EGR flow estimator is identified as the most critical factor, which could lead to black smoke formation. This issue could be prevented with better sensor calibration or by using a differential pressure sensor in the estimator instead of two absolute pressure sensors. Errors in the parameters of the flow estimators do not affect the performance as much. This is a useful result because, for a newly built engine, the right parameters of the flow estimators might be difficult to obtain.

Keywords: Split-range control; Exhaust Gas Recirculation; Marine pollution; Engine control

1 Introduction

Developing a clean and efficient transportation sector is one of the most important goals for any society. Road transport started to define more strict emission limits of CO_2 and other pollutants several decades ago. While marine freight began to be regulated later, but in the past years, significant steps have been taken to reduce its environmental impact. The latest is the stricter Tier III emission limit, which enforces a substantial NO_x reduction for vessels built after January 2016 in certain coastal NO_x Emission Control Areas (NECAs), see International Maritime Organization (2013).

One method to reduce the thermal NO_x formed during the combustion is Exhaust Gas Recirculation (EGR). By recirculating burned gases back into the cylinders, the heat capacity of the air is increased which results in lower cylinder peak temperatures and thus less NO_x formation. EGR has been widely investigated in the automotive sector, e.g., Nieuwstadt et al. (2000); Ammann et al. (2003) among many more, but it has only recently been introduced in large two-stroke diesel engines.

Maintaining a high EGR rate when the vessel is manoeurving in a NECA without smoke formation is a challenging task for the current EGR controllers. The reduced oxygen availability during EGR operation limits the amount of fuel that can be burned without visible black smoke formation. This issue together with the industry trend to downsize the engines for fuel economy can reduce the vessel manoeuvrability. Moreover, the oxygen measurement contains inherent delays due to a required gas extraction process, which caused the original PI feedback to perform poorly in these situations. Hence, better EGR controllers that more appropriately handle these acceleration scenarios are crucial for the emission reduction and introduction of EGR on marine diesel engines.

The controller developed in Nielsen et al. (2017b), that uses an adaptive feedforward (AFF) algorithm, showed to have a great potential to improve the acceleration performance during vessel engine testing. However, before the proposed solution can be adopted widely to more EGR engines, further testing has to be carried out to verify the robustness of the complete installation. Since engine testing is limited by the amount of available EGR engines built and also due to high costs of vessel testing, a full vessel and EGR engine model was developed in Llamas

Authors' Biographies

Xavier Llamas is currently a PhD student at Linköping University. His principal research topic is about modelling and control of EGR on marine two-stroke diesel engines. Moreover, he is also interested in modelling and control of turbocharged combustion engines for road vehicle applications.

Prof. Lars Eriksson is a professor of vehicular systems at the Department of Electrical Engineering, Linköping University. His research interests are modelling, simulation and control of vehicle propulsion systems where he has a special interest in issues related to internal combustion engines and vehicle powertrains for clean and efficient transportation.

http://doi.org/10.24868/issn.2631-8741.2018.009

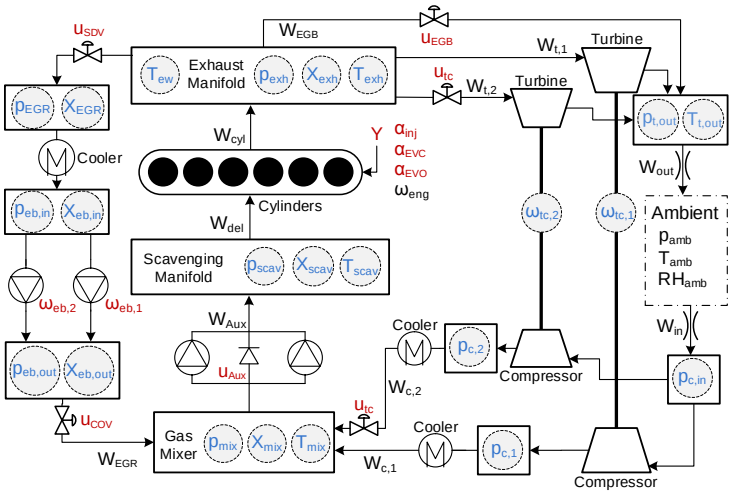

Figure 1: Modelled engine with the model states and control inputs.

and Eriksson (2017) to give a virtual engine and ship that can help identify potential problems during vessel manoeuvring transients.

A new approach for the EGR flow controller that tracks the AFF flow setpoint output is described in this study. The complete simulation model is used to analyse controller performance and this analysis identifies the low load area during ship accelerations as the most problematic case. This issue is further studied by introducing errors in the flow estimator used by the controller at low loads with the purpose to analyse controller robustness. As a result, it is shown that sensor bias can be problematic and lead to the formation of black smoke, while parameter uncertainty has a lesser effect. Increasing the EGR blower flow capacity at low loads is also identified as a factor that has potential to improve the low load EGR control performance.

2 Engine and Ship Models

The studied container ship is powered by a MAN Diesel & Turbo uniflow two-stroke diesel engine with EGR system for Tier III operation. The engine has six cylinders with 3.45 m stroke and 0.8 m bore. At 73.9 rpm it can deliver a maximum rated power of 23 MW.

The engine is modeled following a Mean Value Engine Model (MVEM) approach, where the dynamics are given by the filling and emptying of the different control volumes together with the turbocharger speed dynamics. The cylinders are modeled using a fast analytic cylinder pressure model that captures the influence of the fuel injection and valve timings. Figure 1 contains a diagram of the modeled engine. The rectangles represent the control volumes with its corresponding states inside. The main mass flows are written in the diagram together with the control inputs. The MVEM is implemented in Simulink, and it has 41 states and 10 control inputs. Note that the mass fractions, X, contain one state for each of the four considered species, i.e., $[O_2, CO_2, H_2O, SO_2]$. The complete ship model is completely described, parameterised and validated using real ship measurement data in Llamas and Eriksson (2017).

3 Engine Controller

The engine can operate in four distinct Engine Running Modes (ERM), depending whether the secondary turbocharger is working and whether one or two EGR blowers are running. Here only the fourth ERM is studied, which corresponds to both EGR blowers running and the secondary turbocharger deactivated by closing the cut-out valve, u_{tc}. The EGR Shut Down Valve, u_{SDV}, is open if the engine is operating with EGR and closed otherwise. The fourth ERM is capable to run in any engine load. The cylinder control inputs $(\alpha_{inj}, \alpha_{EVO}, \alpha_{EVC})$ and the EGB valve are controlled here depending on the current ERM and Load, which may not entirely coincide with the real engine control. Finally, the auxiliary blowers are enabled and disabled if the scavenging pressure is below or above a certain value respectively. An overview of the vessel model with the speed governor, the fuel limiter and the EGR controller is shown in Figure 2. The same ordered blower speed, ω_{eb} is applied to both EGR blowers.

3.1 Engine Speed Governor

The governor controls the engine speed to follow the ordered speed setpoint by adjusting the fuel index signal, Y_{gov}. The governor is modelled as a PI controller, see Xiros (2002). During accelerations, the governor ordered fuel index is usually limited to protect the engine. To prevent the controller from winding up while its output is

http://doi.org/10.24868/issn.2631-8741.2018.009

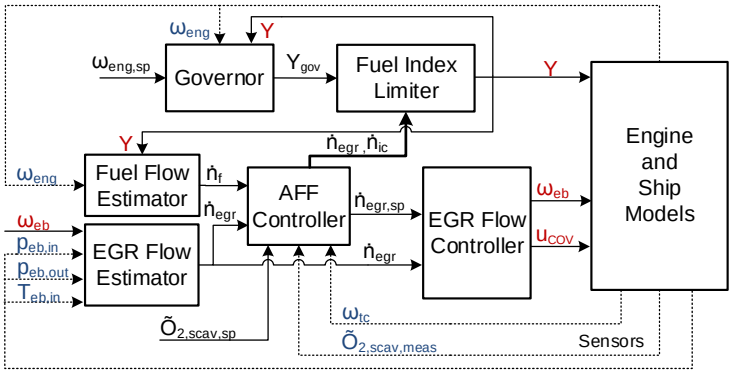

Figure 2: Diagram of the connections between the governor, the fuel index limiters, the EGR controller and the engine and ship models. The diagram shows the primary signals in solid lines and the sensors using dashed lines.

saturated, a tracking term is included as suggested in Åström and Hägglund (2006). The speed governor is defined as

$$Y_{gov} = K_{gov}\, e_\omega + \left(\frac{K_{gov}}{T_{i,gov}} e_\omega + \frac{1}{T_{t,gov}} (Y - Y_{gov}) \right) \frac{1}{s} \tag{1}$$

where e_ω is the difference between the ordered and the current engine speeds. The parameter K_{gov} is the controller gain, $T_{i,gov}$ is the integration time and $T_{t,gov}$ is the tracking time. Note that when the fuel index is not saturated, $Y = Y_{gov}$, and the tracking term in (1) is zero.

3.2 EGR controller

The EGR controller is based on molar flows, $\dot{n}$, instead of mass flows to be able to use the measured volumetric oxygen fraction directly. The AFF controller sets the current EGR flow setpoint to follow a certain oxygen reference in the scavenging manifold. The EGR flow setpoint is then tracked by the EGR flow controller to define the blower speed and COV valve position. The different controller blocks can be seen in Figure 2. The fuel molar flow estimate $(\dot{n}_f)$ is based on a linear function of engine speed and fuel index value, more details can be found in Nielsen et al. (2017c). The EGR molar flow estimate $(\dot{n}_{egr})$ is based on an elliptical model, fitted to the single measured speed line using the nondimensional flow and head coefficients, Φ and Ψ respectively. The model is defined as

$$\Phi = a \left(1 - \left(\frac{\Psi}{b} \right)^n \right)^{\frac{1}{n}} \tag{2}$$

with tree parameters a, b and n. The nondimensional coefficients are defined as

$$\Phi = \frac{\dot{n}_{egr} T_{eb,in} R}{p_{eb,in}\, \omega_{eb}\, 4 r_{eb}^3} \tag{3}$$

$$\Psi = \frac{c_{p,eb} T_{eb,in}}{\omega_{eb}^2 r_{eb}^2} \left(\Pi_{eb}^{\frac{\gamma-1}{\gamma}} - 1 \right) \tag{4}$$

where r_{eb} is the blower radius and the thermodynamical parameters $(R, \gamma, c_{p,eb})$ are taken as constants.

The key equation originally described in Nielsen et al. (2017c) to create the feedforward part of the AFF controller is repeated here for completeness. With the following definitions

$$d = [\dot{n}_f \;\; \omega_{tc}]^T, \quad u = \dot{n}_{egr} \tag{5}$$

and simplifying the gas transport and mixing dynamics, the volumetric oxygen concentration in the scavenging manifold can be computed as

$$g(\theta, d, u) = \tilde{O}_{2,a} - \frac{(1 + \frac{y}{4}(\tilde{O}_{2,a} + 1))\dot{n}_f \dot{n}_{egr}}{(\theta\beta(\omega_{tc}) + \frac{y}{4}\dot{n}_f)(\theta\beta(\omega_{tc}) + \dot{n}_{egr})} \tag{6}$$

where $\tilde{O}_{2,a}$ is the constant molar oxygen fraction of air, y is the constant total ratio of hydrogen to carbon in the fuel. Note that some of the assumptions taken in Nielsen et al. (2017c) to derive (6), are not fulfilled in the MVEM used here. The model structure has changed slightly, a new control volume, named gas mixer, is defined. The gas mixer is connected to the scavenging manifold through the auxiliary blowers. Moreover, the gas mixing dynamics

http://doi.org/10.24868/issn.2631-8741.2018.009

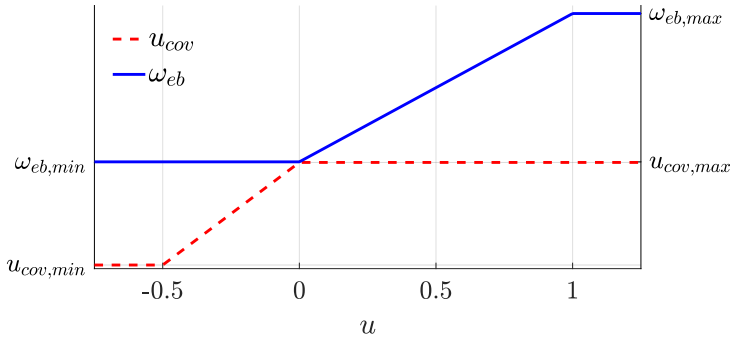

Figure 3: Split-range control diagram of the two actuator outputs depending on the PI controller output.

in the EGR loop have been considered including three control volumes. Furthermore, the coolers contain models for the Water Mist Catchers (WMC). Its main function is to remove the condensed water in the flows, and thus they alter the oxygen concentrations slightly.

The molar flow delivered by the main compressor cooler is computed as

$$\dot{n}_{ic} = \theta\beta(\omega_{tc}) \tag{7}$$

where $\beta(\omega_{tc})$ is a second order polynomial of the turbocharger speed. The parameter θ is adjusted with the adaptation algorithm from Nielsen et al. (2017a) that guarantees oxygen setpoint convergence. The adaptation law is defined as

$$\hat{\theta} = k\left(\tau\tilde{O}_{2,scav,meas+}\int \tilde{O}_{2,scav,meas} - g(\hat{\theta},d,u)\mathrm{dt}\right) \tag{8}$$

with $k > 0$, and the sensor and gas mixing dynamics represented by τ, more details can be found in the original publication Nielsen et al. (2017a). The adaptation uses the oxygen measurement together with the model for the scavenging oxygen concentration (6), to update $\hat{\theta}$. Finally, the EGR molar flow setpoint, $\dot{n}_{EGR,sp}$, is obtained by inverting (6), based on the current molar flow estimates and the desired oxygen concentration setpoint. Experimental results of the controller operating in a container ship and a convergence proof of the AFF are available in Nielsen et al. (2017b).

A new EGR flow controller that tracks the EGR flow setpoint is introduced in this study. In normal operation, the blower speed is used to control the EGR flow. If the lower blower speed limit is reached, the COV valve is used to reduce the flow further until the blower speed can retake control. To avoid controllability problems, a single PI controller is used to control both actuators using a split-range control approach, see Åström and Hägglund (2006). The static relationship between the PI controller output and the actuated signals is depicted in Figure 3. The blower speed limits are constant values, the maximum valve position is 1, and $u_{cov,min}$ depends on the current engine load. The PI controller is defined as

$$v = K_{egr}\, e_{\dot{n}} + \left(\frac{K_{egr}}{T_{i,egr}} e_{\dot{n}} + \frac{1}{T_{t,egr}}(u - v)\right)\frac{1}{s} \tag{9}$$

where the error, $e_{\dot{n}}$, is the difference between the EGR molar flow setpoint and the estimated flow. The PI controller output, u, is limited to the defined controller range $[-0.5, 1]$, see Figure 3. The signal v is the PI controller output before the previously mentioned limitation. Due to this output saturation, the PI controller contains an anti-windup term with constant tracking value $T_{t,egr}$, as in (1). Quicker and wider changes in the actuated signals are required at low engine loads. To obtain good controller performance, the PI gain is scaled to have larger gains at low loads using the scavenging pressure signal as follows

$$K_{egr} = \frac{K}{p_{scav}\cdot 10^{-5}} \tag{10}$$

with the pressure in Pa. Then, K and $T_{i,egr}$ are fixed constant values. The actuator outputs are calculated using the limits as

$$\omega_{eb} = \frac{\omega_{eb,max} - \omega_{eb,min}}{1}\max(0,u) + \omega_{eb,min} \tag{11}$$

$$u_{cov} = \frac{u_{cov,max} - u_{cov,min}}{0.5}\min(u,0) + u_{cov,max} \tag{12}$$

The asymmetry in the defined control range between both actuators has the purpose of establishing suitable control gains for each actuator, e.g., the blower speed gain from the flow error, $e_{\dot{n}}$, is substantially larger due to the speed units compared to the valve normalised position.

http://doi.org/10.24868/issn.2631-8741.2018.009

3.3 Fuel Index Limiters

The injected mass flow is usually limited in various operating situations to prevent engine damage. This is done by specifying an upper value to the fuel index signal, see Xiros (2002). A new Dynamic Limiter Function (DLF) has been proposed in Vejlgaard-Laursen and Olesen (2016), to ensure better acceleration capacity of vessels with downsized engines. This limiter consists of two parts, one that limits the maximum amount of fuel based on an estimate of the trapped air mass in the cylinders and a lower lambda limit, Y_{LA}, and another that limits the fuel to protect the engine from too extreme torsional vibrations, Y_Q. The DLF also controls the injection and exhaust valve timings for faster transients. However, this is not implemented in this paper but could be included by defining specific control laws for α_{inj}, α_{EVC}, and α_{EVO}.

For engines with EGR, the oxygen concentration is lower since the recirculated exhaust gas replaces some of the fresh air in the scavenging receiver. Hence, the amount of fuel that can be burned during accelerations depends not only on the trapped mass but also on the oxygen concentration of that mass. A correction needs to be applied to Y_{LA} to prevent the engine of producing black smoke from incomplete combustion. The oxygen/fuel limiter, Y_{LOM}, described in Nielsen et al. (2016), does this correction by making use of the scavenge oxygen equation (6) to correct the DLF limiter when EGR is being used. Thus, the ordered fuel index going to the engine is calculated as

$$Y = \min(Y_{gov}, Y_{LOM}, Y_Q) \tag{13}$$

4 Results

The governor and EGR controller are investigated under different scenarios to analyse its performance. Moreover, the controller robustness is also examined by adding disturbances to the flow estimators inputs and parameters. Each figure contains the cylinder lambda value, λ_o, and the lambda lower limit for smoke formation, λ_{lim}, so it is easy for the reader to assess whether or not smoke will occur in each case.

4.1 Acceleration Scenarios

Three consecutive increasing engine speed steps have been simulated, the main signals and controlled inputs are shown in Figure 4. These speed steps correspond to engine load increases from 9 % to 90 %. Note that it is not common to reach high engine loads with the EGR system active, but the engine is capable to do so with a single turbocharger. After an initial transient, the oxygen level converges to the desired setpoint for all steps. The convergence is connected to the adaptation parameter, $\hat{\theta}$, and it is achieved once a stable value is reached. The bottom plot of Figure 4 shows the EGR control inputs and the engine load. For the first speed step, the blower speed reaches its lower limit, and the COV valve has to be actuated to reduce the flow. The lowest speed step also has the largest oxygen setpoint deviation at the start of the step, initially drops under 16% and when the COV valve is actuated it crosses the setpoint. After that, the blower speed has to be increased again until it reaches its limit, this shows that EGR blowers with larger flow capacity at low loads would improve the controller performance.

This fast overshoot in the first step is a direct consequence of the quick feedforward setpoint change. The feedforward is built by simplifying the model dynamics and thus assumes that changes in the exhaust flow concentrations have a rapid impact on the scavenging concentration. This takes a long time at low loads due to the slower turbocharger dynamics. This issue can be observed in the zoom-ins of the first two steps shown in Figure 5. The model from (6) predicts a quick oxygen drop in the first step due to the rapid fuel flow increase. If the corresponding EGR flow setpoint was followed perfectly, the overshoot in the oxygen value would be even larger, as can be seen in Figure 6 for the baseline case. Once the adaptive parameter starts to be influenced by the delayed oxygen measurement, the oxygen value reaches the setpoint. For the second load step, this issue is not as critical as can be seen on the right side of Figure 5. However, this behaviour at low loads could be problematic if, for example, the flow estimates are biased, which is further investigated in the next section.

4.2 Controller Robustness Simulations

The first speed step from the previous section is first investigated by biasing the EGR flow input signals. Results with a 3% increase and decrease on the inlet pressure together with band limited white noise added to the blower inlet temperature signal are shown in Figure 6. The added noise is exaggerated by using a standard deviation of $10\,K$. Figure 6 also contains, as a baseline, the case without EGR blower speed limits so that it is easier to compare what would be the best case. The first information that can be extracted is that for the noisy temperature signal, the performance is not substantially reduced. The worst implication is that the fuel index limit calculation is affected by the noise in the EGR flow estimate which results in the lambda value crossing the limit. Similar results have been observed by applying noise to the blower pressure signals, and in all cases, the issue can be prevented with an appropriate filter. The biased pressure cases show more relevant results. With a higher measured inlet pressure, the controller overestimates the EGR flow. This produces an overshoot in the oxygen value and a slightly slower acceleration in the beginning due to a more restrictive fuel limiter.

http://doi.org/10.24868/issn.2631-8741.2018.009

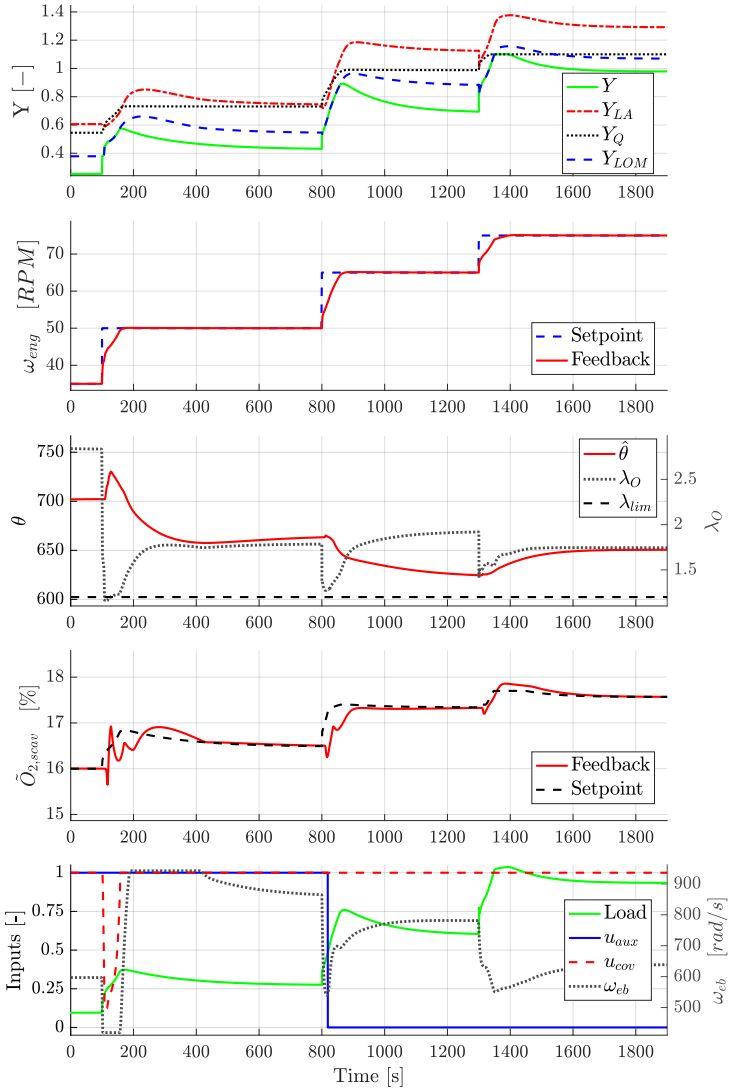

Figure 4: EGR and fuel controller performance during three consecutive engine speed steps. Note that the λ and ω_{eb} have the axis in the right side of the figure.

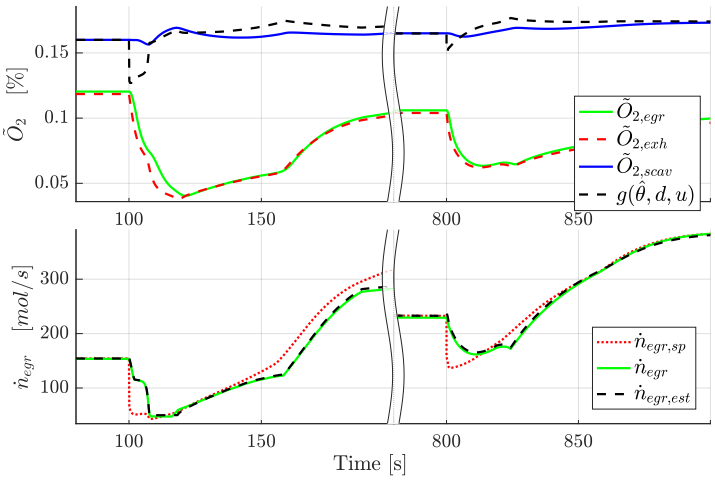

Figure 5: Oxygen Dynamics and EGR molar flows during the two first engine speed steps from Figure 4.

http://doi.org/10.24868/issn.2631-8741.2018.009

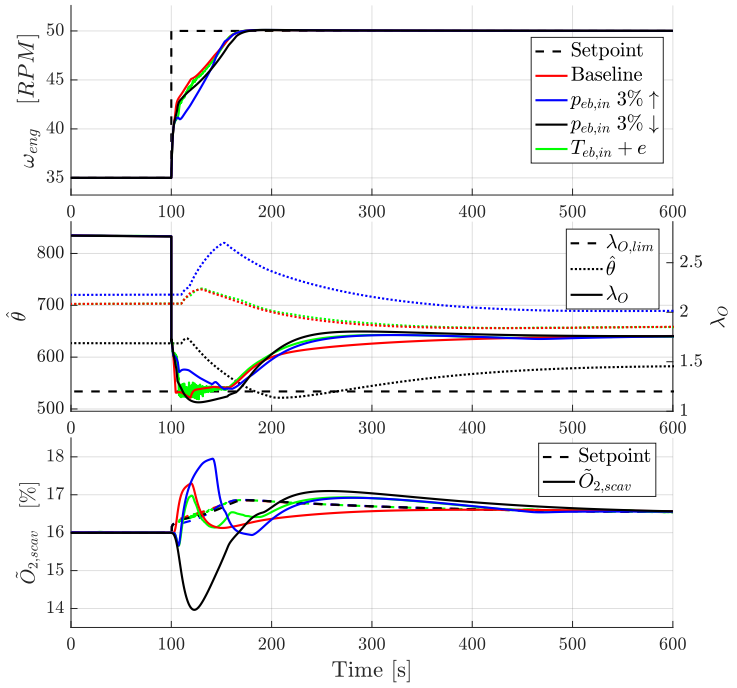

Figure 6: Low load speed step results for disturbances in the inlet pressure of the EGR flow estimator and noise added to the inlet temperature of the EGR blower. Note that the color legend of the first subplot is maintained to differentiate the different cases thoughout the figure. Only the style of the line is included in the rest of the legends.

On the other hand, with a lower measured inlet pressure, the results are the opposite. The EGR flow estimator is working with higher pressure ratios which correspond to an underestimate of the EGR flow. The controller initially expects the oxygen to be higher due to the low EGR flow, which results in a lower oxygen concentration together with a lambda that crosses the limit value. The blower response along with the estimator are shown in Figure 7, where it is seen that a 3% decrease in inlet pressure moves the operating path of the estimator substantially due to the relatively flat blower speed lines in this region. To avoid that the estimator ends up at zero flow, which would have even worse implications for the control performance, a lower flow limit is used in the estimator. The limit is implemented as a saturation of the head parameter, see (14), before evaluating equation (2), and it is depicted in Figure 7 in the pressure ratio-corrected flow plane.

$$\Psi = \min(0.99 \cdot b, \Psi) \tag{14}$$

Similar results as those described above are obtained when biasing the other flow estimator input signals, however, to get similar oxygen deviations, the bias in the blower inlet temperature or turbocharger speed has to be substantially larger than 3%. For the case of blower outlet pressure, similar results are obtained since it influences the pressure ratio and thus moves the operating point of the blower in the same manner as the inlet pressure case. The simulations also show that the sensor bias undesired effects can be significantly reduced by changing either the inlet or the outlet absolute pressure sensor for a differential pressure sensor type. Then, the unmeasured inlet or outlet pressure is computed with the remaining absolute pressure sensor signal plus or minus the measured differential pressure. With this measurement setup, a much higher bias than 3% is required to reach the same undesired effect, which should not happen in the real controller setup.

Further investigations are carried out by modifying the parameters of the flow estimate models. The fuel flow model parameters are increased and decreased by 15% to obtain both over and underestimation of the fuel flow. The EGR flow estimate model is used with the parameters corresponding to the most closed and the most open blower diffuser positions. Closing the blower diffuser vanes results in less flow, and opening them has the contrary effect. Note that the diffuser position in the engine model is fixed at the middle position. Results are shown in Figure 8. As can be observed, the oxygen deviation from the setpoint is less pronounced than for the previous case where the $p_{eb,in}$ was biased. All four cases have little effect on the in-cylinder lambda value, which remains quite similar. This is a valuable result because, in the real application, it can be difficult to verify whether or not the parameters of the flow estimators are accurate. When the EGR controller is calibrated for a new engine, tuning the EGR estimator from the manufacturer EGR blower map and the fuel estimator from stationary fuel consumption measurements during the engine shop test should be sufficient to obtain a good performance.

http://doi.org/10.24868/issn.2631-8741.2018.009

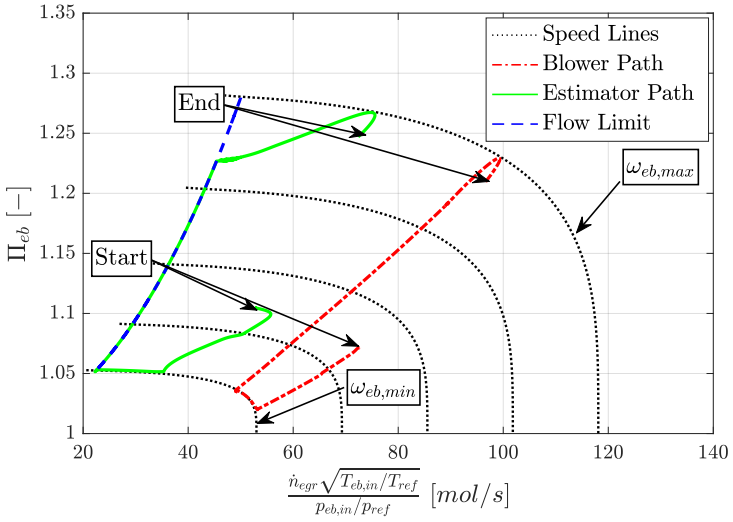

Figure 7: Real blower and flow estimator operating paths in the pressure ratio vs corrected molar flow plane. It corresponds to the $p_{eb,in}$ 3% ↓ case from Figure 6.

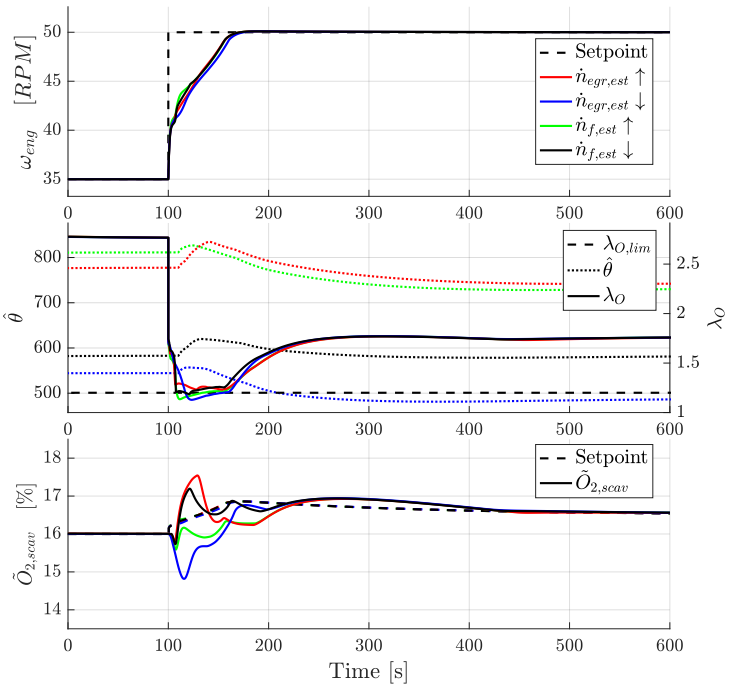

Figure 8: Low load speed step results for under and overestimation of EGR and fuel flows in the EGR controller. Note that the color legend of the first subplot is maintained to differentiate the different cases thoughout the figure. Only the style of the line is included in the rest of the legends.

http://doi.org/10.24868/issn.2631-8741.2018.009

5 Conclusions

The AFF controller together with the proposed EGR flow controller is shown to prevent smoke formation due to incomplete combustion during ship acceleration simulations at different loads. Having EGR blowers with more flow capacity at low loads would be useful for improving the oxygen control performance since the controlled speed hits the lower and upper limits. Moreover, it has been identified that simplifying the dynamics of the AFF inverted model has a substantial impact at low loads where the engine air path dynamics are slower. If the controller flow estimates are accurate, this issue does not impact the control performance substantially. However, when sensor bias is introduced to the EGR blower inlet pressure, the controller performance is affected due to the shift in the operating region of the EGR flow estimate model. This is identified as the most sensitive case, since underestimating the EGR flow could lead to the formation of black smoke during the acceleration. This undesired effect can be prevented by proper sensor calibration or by using a differential pressure sensor in combination with an absolute pressure sensor in the EGR flow estimator. On the other hand, the simulations show that errors in the parameters of the fuel and EGR flow estimators have a lesser effect on the oxygen tracking performance. This is an important result since correctly parameterising the flow estimators could be difficult for a given engine.

Acknowledgement

This project has received funding from the European Union's Horizon 2020 research and innovation programme under grant agreement No 634135.

MAN Diesel & Turbo and in particular Kræn Vodder Busk are greatly acknowledged for the suggestions and for the help in setting up the EGR controller.

References

Ammann, M., Fekete, N. P., Guzzella, L., Glattfelder, A. H., 2003. Model-based control of the VGT and EGR in a turbocharged common-rail diesel engine: Theory and passenger car implementation. In: SAE Technical Paper 2003-01-0357. SAE International.

Åström, K. J., Hägglund, T., 2006. Advanced PID Control. ISA - Instrumentation, Systems, and Automation Society.

International Maritime Organization, 2013. MARPOL: Annex VI and NTC 2008, 2013: with Guidelines for Implementation. IMO.

Llamas, X., Eriksson, L., 2017. Control-oriented modeling of two-stroke diesel engines with EGR for marine applications. Proc. Inst. Mech. Eng. M: Journal of engineering for the maritime environmentSubmitted.

Nielsen, K. V., Blanke, M., Eriksson, L., 2017a. Adaptive observer for nonlinearly parameterized hammerstein system with sensor delay–applied to ship emissions reduction. IEEE Transactions on Control Systems Technology.

Nielsen, K. V., Blanke, M., Eriksson, L., Vejlgaard-Laursen, M., 2016. Diesel engine control system to meet strict emission requirements while maintaining full ship manoeuvring capability. Applied EnergySubmitted.

Nielsen, K. V., Blanke, M., Eriksson, L., Vejlgaard-Laursen, M., 2017b. Adaptive feedforward control of exhaust recirculation in large diesel engines. Control Engineering Practice 65, 26 – 35.

Nielsen, K. V., Blanke, M., Eriksson, L., Vejlgaard-Laursen, M., 2017c. Control-oriented model of molar scavenge oxygen fraction for exhaust recirculation in large diesel engines. ASME. J. Dyn. Sys., Meas., Control. 139 (2).

Nieuwstadt, M., Kolmanovsky, I., Moraal, P., Stefanopoulou, A., Jankovic, M., 2000. EGR-VGT control schemes: experimental comparison for a high-speed diesel engine. IEEE Control Systems Mag. 20 (3), 63–79.

Vejlgaard-Laursen, M., Olesen, H., 2016. Controlling tier III technologies. In: 28th CIMAC World Congress on Combustion Engine.

Xiros, N., 2002. Robust Control of Diesel Ship Propulsion. Springer-Verlag London.

Nomenclature

$\tilde{O}_2$	Oxygen Molar Fraction
$\dot{n}$	Molar flow
P	Power
R	Gas Constant
T	Temperature
W	Mass Flow
X	Mass Fraction
Y	Fuel Index

http://doi.org/10.24868/issn.2631-8741.2018.009

c_p	Specific heat at constant pressure
e	Error
p	Pressure
u	Input signal
r	Radius

Greek Symbols

α	Crank Angle
γ	Specific heats ratio
ω	Rotational speed
Φ	Flow coefficient
Π	Pressure ratio
Ψ	Head coefficient
$\hat{\theta}$	Adaptive parameter
λ_o	Oxygen to fuel ratio

Subscripts

a	Air
aux	Auxiliary Blower
c	Compressor
cov	Cut-Out Valve
cyl	Cylinder
eb	EGR Blower
eng	Engine
est	Estimated
exh	Exhaust
f	Fuel
gov	Governor
ic	Air Cooler
in	Inlet
inj	Injection
$meas$	Measured
out	Outlet
ref	Reference
$scav$	Scavenging
sp	Setpoint
tc	Turbocharger

http://doi.org/10.24868/issn.2631-8741.2018.009